

Supporting Information

for *Adv. Optical Mater.*, DOI: 10.1002/adom.202203148

Reversible Thermochromic Bismuth Iodide Enabled by
Self-Adjustment

Rui Wen, Yanyan Wang, Xinjie Ma, Yikun Yan, Qi Ma,
Jinpeng Gao, Huaming Sun, Hao Huang,* and Ziwei
Gao**

Supporting Information

Reversible Thermochromic Bismuth Iodide Enabled by Self-Adjustment

Rui Wen,^[a] Yanyan Wang,^{*[a]} Xinjie Ma,^[a] Yikun Yan,^[a] Qi Ma,^[a] Huaming Sun,^[a] Hao Huang^{*[d]} and Ziwei Gao^{*[a,b,c]}

Abstract: Light-harvesting materials with dynamical management of light transmittance hold great promise in smart photovoltaic (PV). Here, we present a novel organic-inorganic halide, $MVBi_2I_8$ ($MV = \text{Methylviologen cation}$), exhibiting reversible thermochromism and constant bandgap of approximately 1.65 eV over a wide temperature range of 77K to 453K, as a candidate. The compound consists of 0-dimensional $[Bi_4I_{16}]^{4-}$ clusters and MV^{2+} cations. And the adjacent $[Bi_4I_{16}]^{4-}$ clusters are in touch with each other, forming a 3-dimensional interaction for the inorganic part. The experimental and theoretical studies reveal that the ionic and covalent interactions in the crystal undergo a self-adjusting process in response to temperature changes. The self-adjustment and electron transfer between inorganic clusters and organic cations enable excellent reversible thermochromism and constant narrow bandgaps over a wide temperature range, which is expected for smart PV windows integrated with information displays and potentially other technologies.

[a] R. Wen, Dr. Y.Y. Wang, X.J. Ma, Y.K. Yan, Q. Ma, Dr. H.M. Sun, Prof. Dr. Z.W. Gao
Key Laboratory of Applied Surface and Colloid Chemistry MOE, Xi'an Key Laboratory of Organometallic Material Chemistry, School of Chemistry and Chemical Engineering

Shaanxi Normal University
Xi'an 710119, P. R. China
E-mail: zwgao@snnu.edu.cn, yyw@snnu.edu.cn

[b] Prof. Dr. Z.W. Gao
School of Chemistry & Chemical Engineering,
Xinjiang Normal University
Urumqi, 830054, P. R. China

[c] Prof. Dr. Z.W. Gao
Research Institute of Comprehensive Energy Industry Technology, College of Chemistry & Chemical Engineering
Yan'an University
Yan'an, 716000, Shaanxi, P. R. China

[d] Dr. H. Huang
Department of Microsystems,
University of South-Eastern Norway,
Borre 3184, Norway
E-mail: huanghao881015@163.com

Table of Contents

Experimental Procedures	
Synthesis.	3
General characterization.	3
X-ray Crystallography.	3
Raman spectra measurement.	3
Optical absorption measurement.	3
Computational methods.	3
Two-point probe conductivity measurements.	4
Photo response measurement.	4
Results and Discussion	
Figure S1. The single crystals SEM image of 1	5
Figure S2. The TG curve of 1	5
Figure S3. The experimental powder XRD patterns of 1	6
Figure S4. The experimental PXRD patterns of the films of 1	6
Figure S5. The electronic band structures of 1 at 150K and RT.	7
Figure S6. The crystal structure of 1 viewing along the [100] direction at 150K.....	7
Figure S7. The DOSs plots of 1 at RT.	8
Figure S8. The UV-vis absorption spectra of the thin film sample of 1 before and after UV Irradiation.....	8
Figure S9. <i>J-E</i> curves of 1 at different temperatures.	9
Figure S10. The <i>I-V</i> and photo-current response curves of tablet and thin film of 1 at RT.	9
Table S1. Crystal data and structure refinements for 1	10
Table S2. Selected bond lengths (Å) and angles (°) for 1	11
References.....	13

Experimental Procedures

Synthesis.

Synthesis of (MV)Bi₂I₈ (1). (MV)Bi₂I₈ was synthesized by a typical solvothermal method. In a Teflon lining, 1 mmol of bismuth iodide (BiI₃), 0.5 mmol of 4,4'-bipyridine and 18mmol of HI (55-58%wt hydroiodic acid) were mixed thoroughly into 10 mL of methanol. The Teflon lining with the mixture was then sealed in a stainless-steel reactor and heated at 120°C for 60h. After the reaction was completed, the reactor was naturally cooled to room temperature. Pure phase of dark-red crystals with block morphology was obtained in the reagent. To remove the excess acid on the crystal surface, we washed the crystals with methanol several times. Then the target product was collected after drying at 60 °C overnight.

Synthesis of drop-coated film of 1. Firstly, **1** was dissolved into a mixed solvent of DMF:DMSO = 4: 1.3 to make a solution. Then, we dropped the solution onto fluorine-doped tin oxide (FTO) glass. And a dark-red film with compound **1** was obtained after annealing the film at 180°C. Powder XRD analysis indicate the purity of the thin film.

Synthesis of spin-coated film of 1. Firstly, **1** was dissolved into a mixed solvent of DMF:DMSO = 4: 1.3 to make a solution. Then, we dropped the solution onto fluorine-doped tin oxide (FTO) glass using spin coating with 4000 rpm. And a dark-yellow film with compound **1** was obtained after annealing the film at 180°C. Powder XRD analysis indicate the purity of the thin film.

General characterization.

Powder X-ray diffraction (PXRD) data were collected on a Bruker D8 Advance diffractometer with Cu K α radiation ($\lambda = 1.5418 \text{ \AA}$). Thermogravimetric analysis (TGA) was carried out on a TA Q1000 analyzer in N₂ with a heating rate of 5 °C min⁻¹ from RT to 800 °C.

X-ray Crystallography.

Single-crystal X-ray diffraction data collections for **1** were conducted on a Bruker SMART APEX II CCD diffractometer (Mo, $\lambda = 0.71073 \text{ \AA}$) by using the θ - ω scan technique at 150 K and 293 K, respectively. The structures were solved by direct methods and refined with a full-matrix least-squares technique within the SHELXL program package.^[1] All non-hydrogen atoms were refined anisotropically. The crystallographic details are provided in Table S1. The structure was checked for missing symmetry elements using the program PLATON,^[2] and no higher symmetry was found. Selected bond distances and bond angles are listed in Table S2. Crystallographic data for the structural analyses have been deposited at the Cambridge Crystallographic Data Center. The crystallographic data for above compounds can be found in the Supporting Information or can be obtained free of charge from the Cambridge Crystallographic Data Centre via http://www.ccdc.cam.ac.uk/data_request/cif. CCDC Numbers: 2168530 (MVBi₂I₈, **1**, 150K), 2094265 (MVBi₂I₈, **1**, RT).

Raman spectra measurement.

Raman spectra of solid-state of **1** with different temperatures was detected by using Microconfocal Laser Raman Spectrometer with specification in Via Reflex under 785 nm laser excitation.

Optical absorption measurement.

Solid-state of **1** diffusion reflectance spectra was detected by using a SHIMADZU UV-3600 UV-Vis-NIR spectrophotometer using BaSO₄ powder as the reflectance reference. The absorption spectra were calculated by reflectance spectra using the Kubelka-Munk function: $F(R) = \alpha/S = (1-R)^2/2R$,^[3] where R is the coefficients for the reflection, α is the absorption and S is the scattering. Meanwhile, the bandgap was calculated by tauc-plot method using function: $(ah\nu)^n = A(h\nu - E_g)$, where a is absorption coefficient, $h\nu$ is incident photon energy, A is energy independent constant and E_g is the optical bandgap. In this equation, the exponent "n" represent the nature of transition. Based on direct bandgap material $n = 2$ while for indirect $n = 1/2$. From result given in Figure S5, the bandgap of compound **1** is indirect so that the n value of 1/2.

Computational methods.

In our calculations, the first-principles calculations of electronic structure, band structures of **1** were carried out to understand the relationship between structure and properties. The total density of states (TDOS) of organic part in the slab was computed by using

the Projector Augmented Wave method (PAW).^[4,5] The exchange correlation functional in these calculations is approximated using generalized gradient approximation (GGA) type Perdew-Burke-Ernzerhof (PBE).^[6,7] We built the initial model based on single crystal structure of **1** and then optimized the structure till the force on every atom is less than 0.01 meV/Angstrom with the cutoff of 500 eV.

Two-point probe conductivity measurements.

For electrical measurements, the powder sample of **1** was compressed into tablets (with diameter of 1.2 cm and thickness of 0.095 cm for **1**). The two undersides of tablets were connected to a source meter (Keithley 2400). The two sides of tablet were painted by conductive silver paste and stick a copper wire coated by silver, respectively. The silver coated copper wire was used as the conductor wire. Current-voltage (*I*-*V*) curves were scanned at various voltage ranges according to the resistance of the single crystals and the sensitivity of the instrument. The conductivity is calculated by the plots of current density versus electric field strength (*J*-*E* curves) based on the following Ohm's law,

$$\sigma = J / E,$$

$$J = I / S,$$

$$E = V / L$$

where σ is the conductivity, *J* is the current density, *E* is the electric field strength, *I* is the current, *V* is the voltage, *S* is the cross-sectional area of the pressed tablets, and *L* is the thickness of the tablets.

Photo response measurement.

Tablets of pressed powder and thin film of **1** were used for the photo response measurement (Figure S11). We use silver paint to make current collectors and to attach the silver-clad copper wires for the tablets. The areas of silver paint are two semicircles, and one narrow strip like area was left without paint which can receive light from the lamp. Since the resistance in this system is as high as about 1011 Ω , contact resistances between tablet sample, silver paint and wires are negligible. For that reason, two-probe measurements were adopted. We used a picoammeter (Keithley 6485) in series with a source meter (Keithley 2400) to detect the small current in this test.^[8] A 300 W solar-simulating Xenon lamp was used as light source. We blocked or unblocked the light and detected the changes in current. A bias voltage of 12 V was used for sample **1**, to separate the signals from the noise of the system.

Results and Discussion

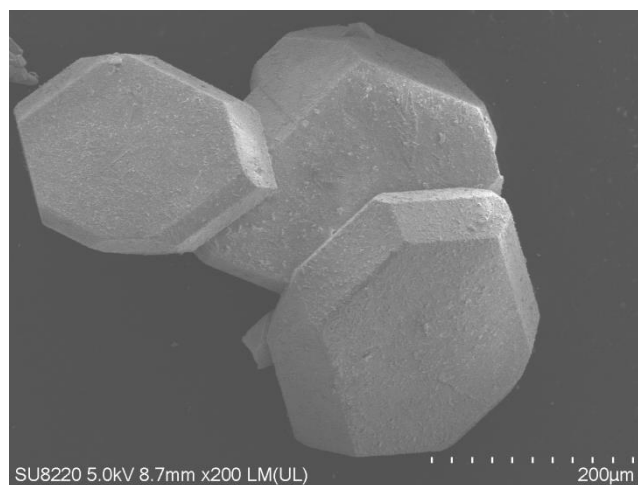


Figure S1. The single crystals SEM image of 1.

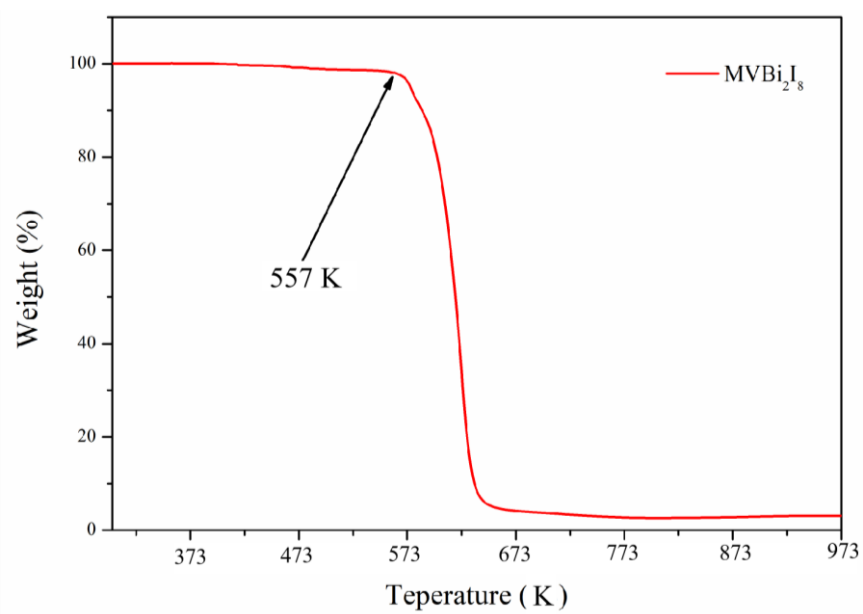


Figure S2. The TG curve of 1.

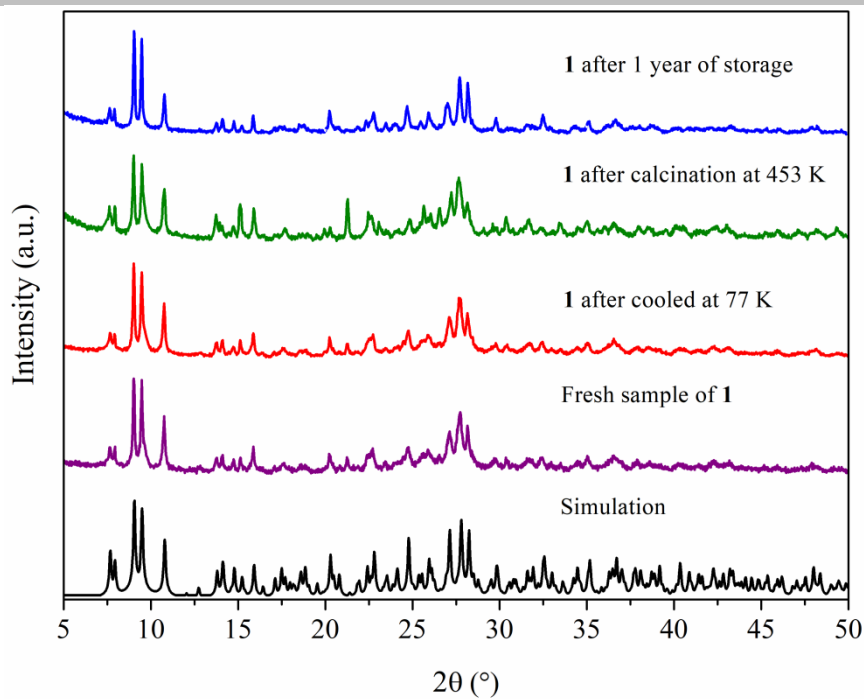


Figure S3. The experimental powder XRD patterns of **1**.

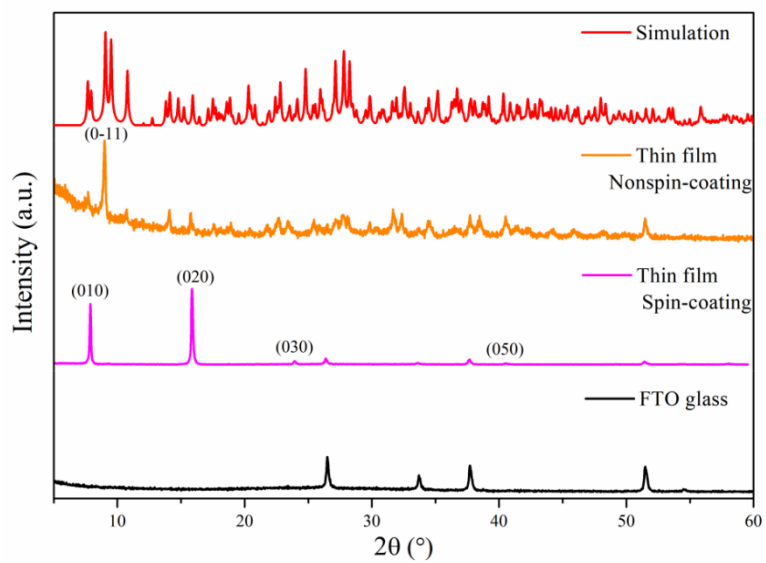


Figure S4. Experimental PXRD patterns of the films of **1**.

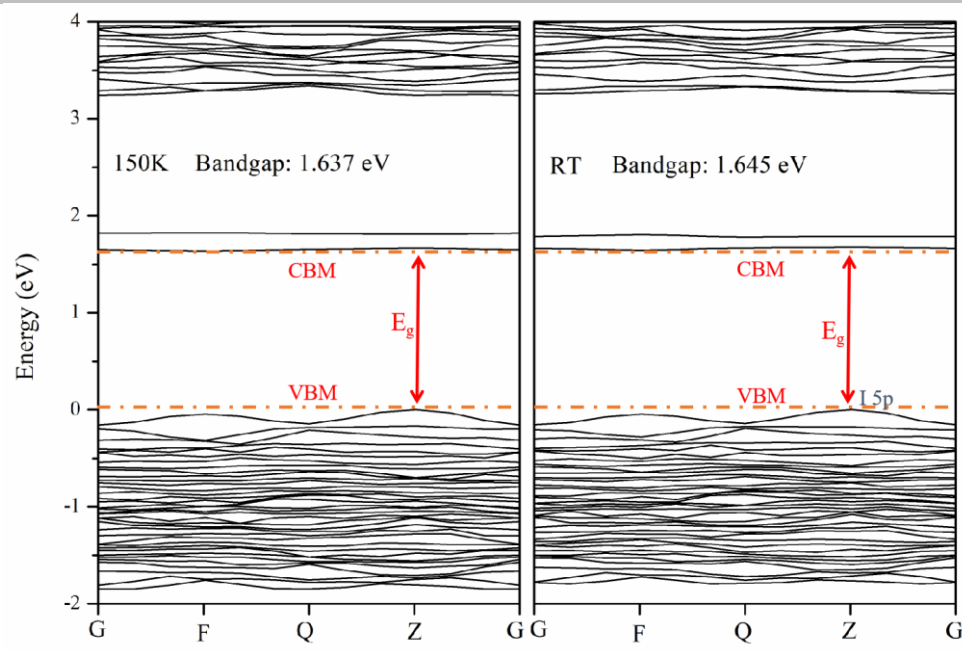


Figure S5. The electronic band structures of 1 at 150K and RT.

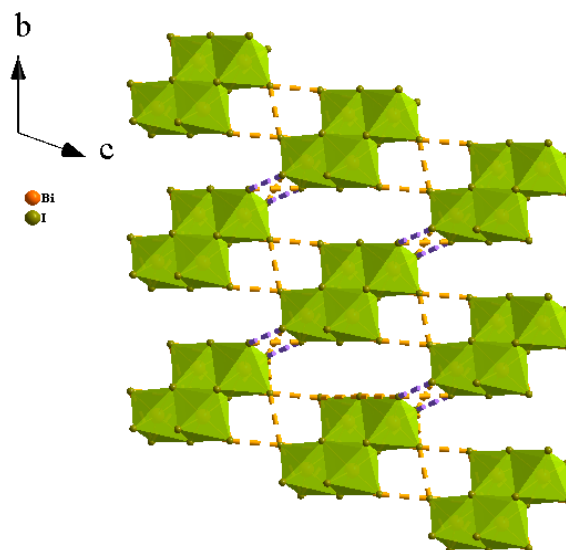


Figure S6. The crystal structure of 1 viewing along the [100] direction at 150K. The purple dashed lines mark the new I...I contacts formed.

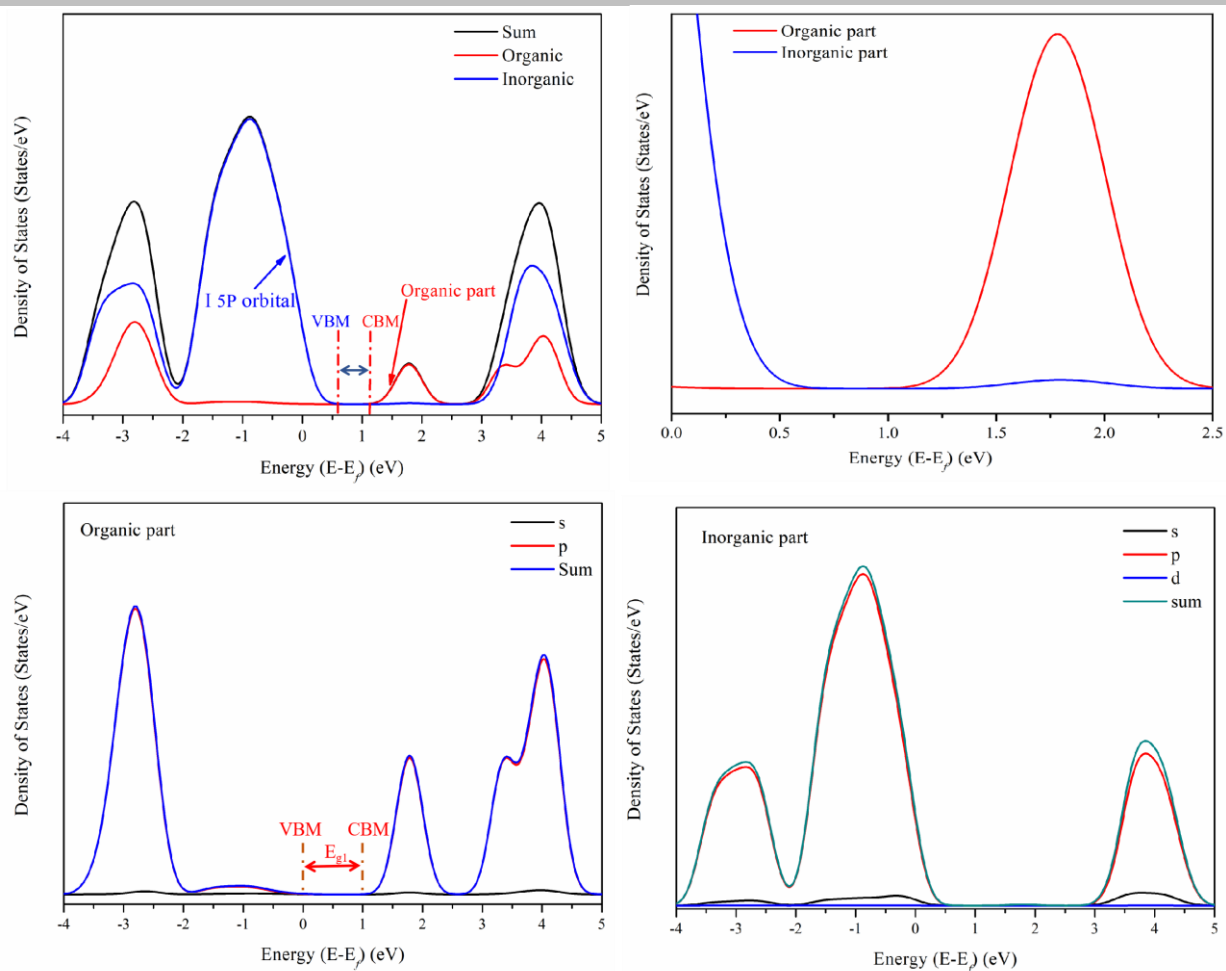


Figure S7. The DOSs plots of 1 at RT.

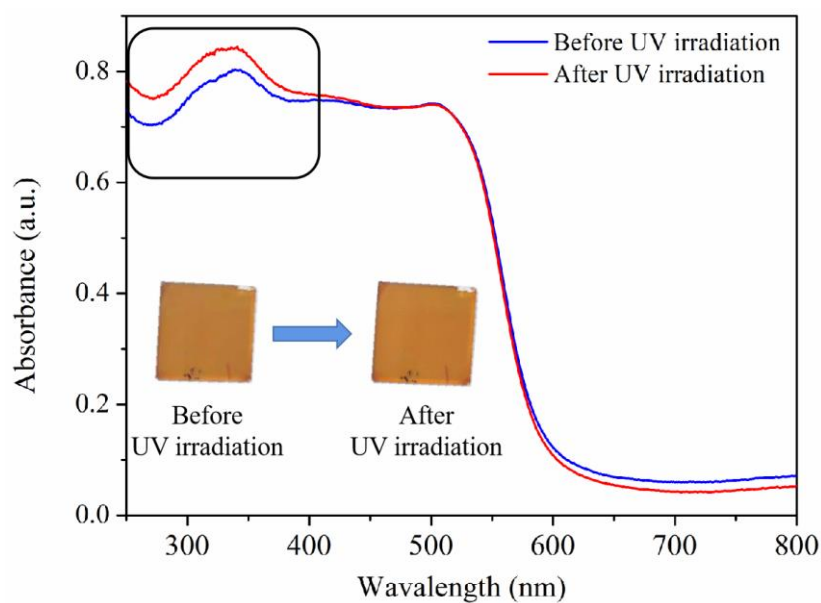


Figure S8. The UV-vis absorption spectra of the thin film sample of 1 before and after UV Irradiation.

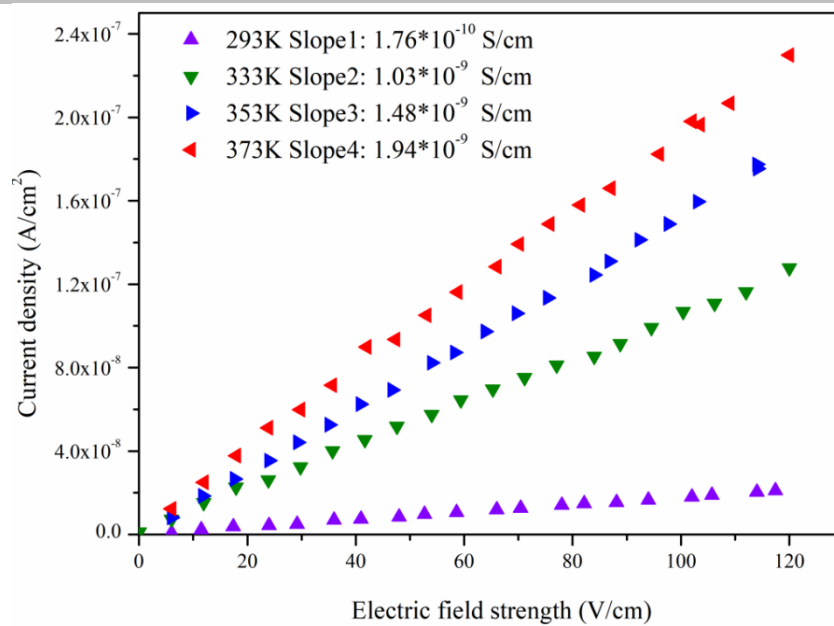


Figure S9. J - E curves of 1 at different temperatures.

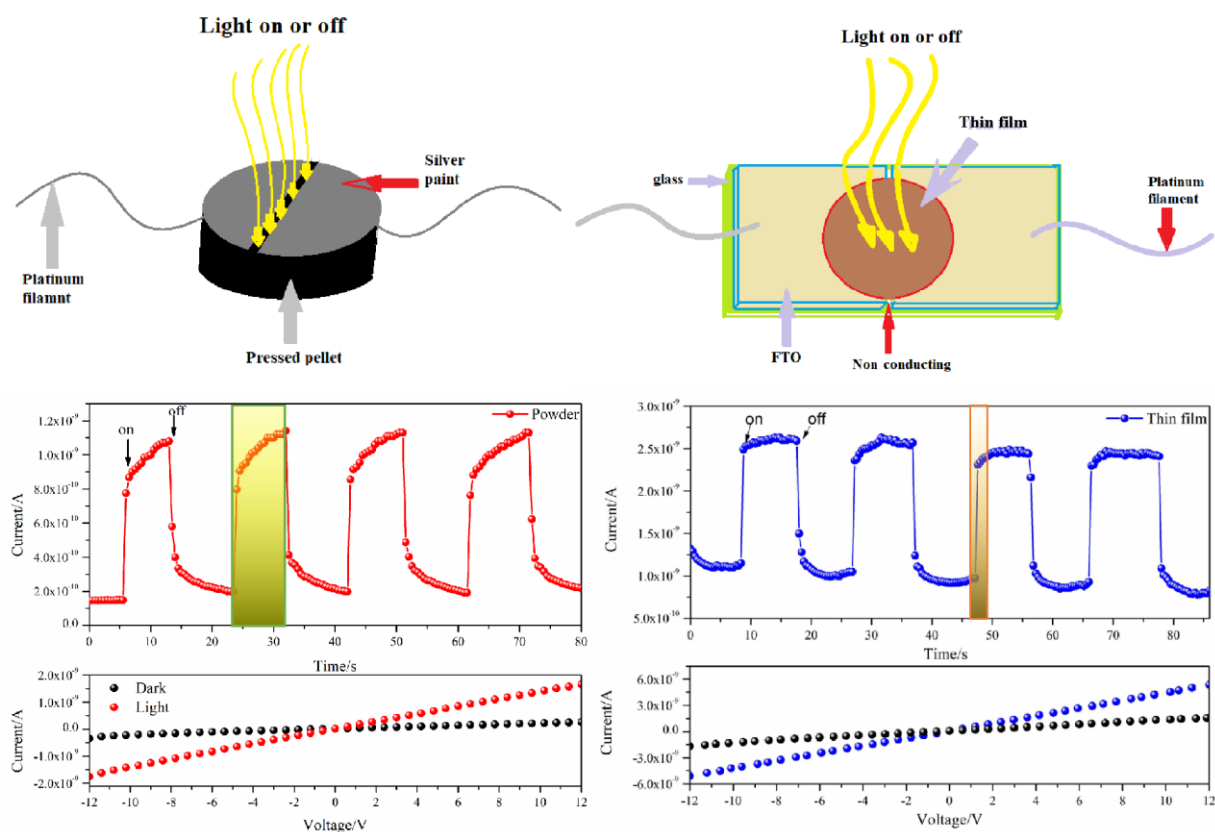


Figure S10. The I - V and photo-current response curves of tablet and thin film of 1 at RT.

Table S1. Summary of crystal data and structural refinements for **1** at RT and 150K.

Compounds	1	
Formula	C ₂₄ H ₂₈ N ₄ Bi ₄ I ₁₆	C ₂₄ H ₂₈ N ₄ Bi ₄ I ₁₆
Formula weight	3238.82	3238.82
Crystal system	Triclinic	Triclinic
Space group	<i>P</i> -1	<i>P</i> -1
Temperature (K)	293(2)	150(2)
<i>a</i> (Å)	10.4284(3)	10.3500(10)
<i>b</i> (Å)	11.8636(4)	11.8687(12)
<i>c</i> (Å)	13.2394(4)	13.2099(13)
α (deg)	104.713(3)	105.600(4)
β (deg)	113.028(3)	112.874(3)
γ (deg)	96.777(3)	96.103(4)
<i>V</i> (Å ³)	1413.87(8)	1398.8(3)
<i>F</i> (000)	1380.0	1380.0
<i>Z</i>	1	1
Absorption coefficient (mm ⁻¹)	21.165	21.394
Reflns collected	51728	55484
Unique reflns	4974	5586
<i>R</i> _{int}	0.0906	0.0583
Data/restraints/parameters	4974/6/219	5586/0/219
Goof on <i>F</i> ²	1.061	1.099
Final <i>R</i> indices [<i>I</i> > 2σ(<i>I</i>)]	<i>R</i> ₁ = 0.0651, <i>wR</i> ₂ = 0.2070	<i>R</i> ₁ = 0.0356, <i>wR</i> ₂ = 0.0956
<i>R</i> indices (all data)	<i>R</i> ₁ = 0.0885, <i>wR</i> ₂ = 0.2290	<i>R</i> ₁ = 0.0361, <i>wR</i> ₂ = 0.0959

Table S2. Selected bond lengths (Å) and angles (°) for **1** at RT and 150K.

293K		150K	
Bi(01)-I(003) ¹	3.3425(16)	Bi(01)-I(003) ¹	3.3532(7)
Bi(01)-I(003)	3.3298(17)	Bi(01)-I(003)	3.3381(8)
Bi(01)-I(004)	3.0603(17)	Bi(01)-I(004)	3.0700(7)
Bi(01)-I(005)	2.9011(17)	Bi(01)-I(005)	2.9110(8)
Bi(01)-I(006)	2.8842(17)	Bi(01)-I(007)	2.8932(8)
Bi(01)-I(007)	3.0800(18)	Bi(01)-I(00A)	3.0847(8)
Bi(02)-I(003)	3.3583(17)	Bi(02)-I(003)	3.3638(7)
Bi(02)-I(004)	3.2701(17)	Bi(02)-I(004)	3.2681(7)
Bi(02)-I(007) ¹	3.3979(18)	Bi(02)-I(006)	2.8947(8)
Bi(02)-I(008)	2.8782(19)	Bi(02)-I(008)	2.8806(8)
Bi(02)-I(009)	2.8684(18)	Bi(02)-I(009)	2.9555(8)
Bi(02)-I(00A)	2.9367(19)	Bi(02)-I(00A) ¹	3.4042(8)
I(003)-Bi(01) ¹	3.3425(16)	I(003)-Bi(01) ¹	3.3532(7)
I(007)-Bi(02) ¹	3.3979(18)	I(00A)-Bi(02) ¹	3.4042(8)
N(00B)-C(7)	1.33(3)	N(00B)-C(00C)	1.345(13)
N(00B)-C(8)	1.36(4)	N(00B)-C(00E)	1.480(16)
N(00B)-C(10)	1.47(4)	N(00B)-C(12)	1.359(15)
C(00C)-C(00F)	1.37(4)	C(00C)-C(00F)	1.377(16)
C(00C)-C(4)	1.41(4)	N(00D)-C(00J)	1.363(14)
C(00C)-C(5)	1.40(3)	N(00D)-C(00K)	1.346(16)
N(00D)-C(1)	1.29(4)	N(00D)-C(17)	1.511(17)
N(00D)-C(9)	1.33(4)	C(00F)-C(00H)	1.392(15)
N(00D)-C(15)	1.59(5)	C(00G)-C(00H)	1.478(15)
C(00E)-C(4)	1.40(4)	C(00G)-C(00I)	1.385(15)
C(00E)-C(1)	1.39(5)	C(00G)-C(19)	1.417(14)
C(00F)-C(7)	1.35(4)	C(00H)-C(18)	1.417(14)
C(4)-C(11)	1.45(4)	C(00I)-C(00J)	1.342(16)
C(5)-C(8)	1.37(5)	C(00K)-C(19)	1.388(17)
C(9)-C(11)	1.35(5)	C(12)-C(18)	1.352(17)
I(003)-Bi(01)-I(003) ¹	84.62(4)	I(003)-Bi(01)-I(003) ¹	84.772(18)
I(004)-Bi(01)-I(003)	86.06(4)	I(004)-Bi(01)-I(003)	86.290(19)
I(004)-Bi(01)-I(003) ¹	88.31(4)	I(004)-Bi(01)-I(003) ¹	87.429(19)
I(004)-Bi(01)-I(007)	173.57(5)	I(004)-Bi(01)-I(00A)	174.44(2)
I(005)-Bi(01)-I(003) ¹	88.20(5)	I(005)-Bi(01)-I(003) ¹	87.83(2)
I(005)-Bi(01)-I(003)	172.52(5)	I(005)-Bi(01)-I(003)	172.39(2)
I(005)-Bi(01)-I(004)	91.64(5)	I(005)-Bi(01)-I(004)	91.58(2)
I(00A)-Bi(02)-I(004)	170.73(6)	I(009)-Bi(02)-I(004)	170.21(2)

I(00A)-Bi(02)-I(007) ¹	93.23(6)	I(009)-Bi(02)-I(00A) ¹	93.01(2)
Bi(01)-I(003)-Bi(01) ¹	95.38(4)	Bi(01)-I(003)-Bi(01) ¹	95.228(18)
Bi(01) ¹ -I(003)-Bi(02)	90.88(4)	Bi(01)-I(003)-Bi(02)	91.918(18)
Bi(01)-I(003)-Bi(02)	92.28(4)	Bi(01) ¹ -I(003)-Bi(02)	89.843(18)
Bi(01)-I(004)-Bi(02)	99.19(4)	Bi(01)-I(004)-Bi(02)	98.90(2)
Bi(01)-I(007)-Bi(02) ¹	94.84(5)	Bi(01)-I(00A)-Bi(02) ¹	93.80(2)

Symmetry transformations used to generate equivalent atoms:

¹1-X,1-Y,1-Z

References

- [1] G. M. Sheldrick, *Acta Crystallogr. Sect. A: Found. Crystallogr.* **2008**, *64*, 112-122.
- [2] A. L. Spek, *J. Appl. Crystallogr.* **2003**, *36*, 7-13.
- [3] J. Tauc, *Mater. Res. Bull.* **1970**, *5*, 721.
- [4] J. P. Perdew, K. Burke, Y. Wang, *Phys. Rev. B* **1996**, *54*, 16533.
- [5] J. Hafner, *J. Comput. Chem.* **2008**, *29*, 2044.
- [6] J. Klimes, D. R. Bowler, A. Michaelides, *Phys. Rev. B* **2011**, *83*, 195131.
- [7] J. Klimes, D. R. Bowler, A. Michaelides, *J. Phys.: Condens. Matt.* **2010**, *22*, 022201.
- [8] M.-Q. Li, Y.-Q. Hu, L.-Y. Bi, H.-L. Zhang, Y. Wang, Y.-Z. Zheng, *Chem. Mater.* **2017**, *29*, 5463–5467.